Molecular Human Reproduction, Vol.00, No.0, pp. 1–12, 2020
doi:10.1093/molehr/gaaa074

molecular human reproduction

ORIGINAL RESEARCH

HMGA2-induced epithelial–mesenchymal transition is reversed by let-7d in intrauterine adhesions

Minmin Song, Chenrui Cao, Zhenhua Zhou, Simin Yao, Peipei Jiang, Huiyan Wang, Guangfeng Zhao *, and Yali Hu *

Department of Obstetrics and Gynecology, The Affiliated Drum Tower Hospital of Nanjing University Medical School, Nanjing, China

*Correspondence address. Department of Obstetrics and Gynecology, The Affiliated Drum Tower Hospital of Nanjing University Medical School, Nanjing, 210008, China. E-mail: yalihu@nju.edu.cn (Y.H.) or E-mail: zhaoguangfeng@njglyy.com (G.Z.)

Submitted on September 18, 2020; resubmitted on October 26, 2020; editorial decision on November 11, 2020

ABSTRACT: Intrauterine adhesions (IUAs), the leading cause of uterine infertility, are characterized by endometrial fibrosis. The management of IUA is challenging because the pathogenesis of the disease largely unknown. In this study, we demonstrate that the mRNA and protein levels of high mobility group AT-hook 2 (HMGA2) were increased by nearly 3-fold ($P < 0.0001$) and 5-fold ($P = 0.0095$) in the endometrial epithelial cells (EECs) of IUA patients (n = 18) compared to controls. *In vivo* and *in vitro* models of endometrial fibrosis also confirmed the overexpression of HMGA2 in EECs. *In vitro* cell experiments indicated that overexpression of HMGA2 promoted the epithelial–mesenchymal transition (EMT) while knockdown of HMGA2 reversed transforming growth factor-β-induced EMT. A dual luciferase assay confirmed let-7d microRNA downregulated HMGA2 and repressed the pro-EMT effect of HMGA2 *in vitro* and *in vivo*. Therefore, our data reveal that HMGA2 promotes IUA formation and suggest that let-7d can depress HMGA2 and may be a clinical targeting strategy in IUA.

Key words: HMGA2 / epithelial–mesenchymal transition / intrauterine adhesions / endometrial fibrosis / let-7d

Introduction

Intrauterine adhesions (IUAs) are the most common cause of uterine infertility. They are characterized by progressive-fibrosis of the endometrium which can induce partial or complete closure of the uterine cavity that is very difficult to treat in severe cases (Yu et al., 2008; March, 2011a,b). Uterine curettage after pregnancy is the main cause of IUA (Hooker *et al.*, 2014). The overall prevalence of IUA in infertile patients is between 2% and 22% (Al-Inany, 2001). A recent systematic review reported that among women with all types of miscarriage, the incidence of IUA ranges from 6% to 30% (Salazar *et al.*, 2017). Although our recent study and other reports suggest that the epithelial–mesenchymal transition (EMT) of endometrial epithelial cells (EECs) is a crucial driver of endometrial fibrosis (Ai *et al.*, 2020; Zhao *et al.*, 2020), the precise mechanism of EMT associated with the pathogenesis of IUA remains largely unexplored.

High mobility group AT-hook 2 (HMGA2), a small non-histone protein of the HMGA family, is an important regulator in EMT of development and neoplasia process (Fusco and Fedele, 2007; Fedele and Fusco, 2010; Macrì *et al.*, 2016). More notably, HMGA2 has been implicated in EMT processes in some fibrotic diseases (Wang *et al.*, 2016a,b; Hou *et al.*, 2018; Zhu *et al.*, 2019). Studies have reported that regulating HMGA2 expression prevented renal fibrogenesis and that loss of HMGA2 weakened EMT in tubular epithelial cells (Wang *et al.*, 2016a,b; Zhu *et al.*, 2019). In addition, HMGA2 was also involved in EMT of pulmonary fibrosis and lens fibrosis through transforming growth factor (TGF)-β signaling pathways (Wang *et al.*, 2016a,b; Hou *et al.*, 2018). The post-transcriptional regulation of HMGA2 expression by the microRNA, let-7d, has gained great attention (Hammond and Sharpless, 2008; Vignali and Marracci, 2020). However, the expression and function of HMGA2 and let-7d in the endometria of IUA patients are unknown.

Here, we demonstrate that HMGA2 was significantly up-regulated and let-7d was down-regulated in endometria of IUA patients. Further research showed that let-7d directly inhibited HMGA2 expression to reverse EMT and we confirmed the regulating role of let-7d/HMGA2 in EEC-EMT in an IUA-like mouse model. Our findings provide a new molecular mechanism of IUA and suggest a novel therapeutic target for its treatment.

Materials and methods

Human endometria collection

Human endometrial samples were obtained from patients with severe IUA or infertility (controls) who underwent hysteroscopy in the Affiliated Drum Tower Hospital of Nanjing University from January

Table I Clinical information of patients.

Items	Control (n = 18)	Intra uterine adhesions (n = 18)	*P*-value
Age (years)	30.11 ± 1.17	30.18 ± 0.43	0.6346
Duration of infertility (years)	1.22 ± 0.10	4.17 ± 1.42	0.0365
Indication	Tubal disease	Severe intrauterine adhesion	
Intrauterine adhesions under hysteroscopy (AFS score)	0	9.35 ± 0.28	<0.0001
Endometrial thickness (mm) (late-proliferative phase)	8.98 ± 0.63	5.25 ± 0.33	0.0001

Values are presented as mean ± SD.
AFS, American Fertility Society.

2014 to December 2016. Informed consents were obtained from all participants. This study was approved by the Ethics Committee of the Nanjing Drum Tower Hospital (No. 2012022).

The age of all participants at the time of entry ranged from 20 to 42 years old. The infertility patients in the control group all had tubal disease with normal ovaries and endometrium diagnosed by hysteroscopy and ultrasonography. The diagnosis of severe IUA patients was based on the scoring standards adopted by The American Fertility Society (1988). The clinical information of all donors is summarized in Table I. Endometrial tissues from all participants were obtained in the late proliferative phase based on 15-18 mm size of dominant follicle (transvaginal ultrasound scan) and a plasma progesterone level <5.5 nmol/l. All enrolled donors did not use hormone medication for at least two menstrual cycles before the samples of their endometria were taken. The acquired endometria were immediately stored in liquid nitrogen or RNAlater (QIAGEN, Dusseldorf, Germany) for subsequent experiments after curettage.

Cell culture and drug treatment

Ishikawa (IK) cells were maintained in Dulbecco's Modified Eagle's Medium: Nutrient Mixture F-12 (DMEM/F-12, Corning, Corning, New York, USA) supplemented with 10% (v/v) fetal bovine serum and 100 U/ml penicillin and 0.1 mg/ml streptomycin at 37°C with 5% CO_2. To successfully induce EMT, IK cells were cultured in serum-free medium overnight before TGF-β1 (PeproTech, cat# 100-21, Rocky Hill, NJ, USA) was added to the medium to a final concentration of 10 ng/ml.

RNA isolation and quantitative real-time PCR (qRT-PCR)

Total RNA was extracted from endometrial tissues or IK cells using TRIzol reagent (Tiangen, China) and measured by Nanodrop spectroscopy (Thermo Scientific, Waltham, MA, USA). Reverse transcription of 1 μg RNA into cDNA was performed according to the PrimeScript™ RT reagent kit (Vazyme, Nanjing, China). qRT-PCR amplification was performed using the ChamQ SYBR® qPCR Master Mix (Vazyme) in a LightCycler 480 machine (Roche, Indianapolis, IN, USA). GAPDH served as internal controls for mRNA normalization and U6 served for miRNAs normalization. The relative RNA level of each gene was determined by the $2^{-\Delta\Delta Ct}$ method. All primer sequences are listed in Supplementary Table SI.

Western blotting

Endometrial tissues or IK cells were lysed using RIPA lysis buffer supplemented with protease inhibitor cocktail (MedChemExpress, NJ, USA) for 30 min on ice. The lysates were centrifuged at 13 800 *g* for 20 min and the clarified protein concentration was measured using a Pierce BCA protein reagent kit (Thermo Scientific). Equal amounts (30 μg) of proteins were electrophoresed on 10% or 15% SDS-polyacrylamide gels, and the same batch of samples were run in the same electrophoresis tank and then simultaneously transferred to polyvinylidene difluoride membranes. After blocking with 5% defatted milk, the membranes were incubated with primary antibodies overnight. After washing with PBST, these membranes were incubated in horseradish peroxidase (HRP)-conjugated secondary antibody (Cell Signaling Technology, Boston, Mass, USA) at a dilution of 1:2000 for 1 h at room temperature. The protein bands were visualized with enhanced chemiluminescence solution (Fdbio science, Hangzhou, China) and quantified using Image J software. GAPDH was run separately and quantified, then used as an internal reference to quantitatively analyze the expression of each protein. The primary antibodies used in this study were listed in Supplementary Table SII.

Hematoxylin and eosin (H&E), Masson and immunohistochemistry staining

The human or mouse endometrial tissues were fixed with 4% paraformaldehyde for 24 h and then embedded into paraffin blocks after dehydration and hyalinization. The paraffin-embedded tissues were cut into 5-mm-thick slices. Tissue sections were stained with hematoxylin and eosin to observe changes in endometrial morphology. Masson staining was performed according to the manual of a kit (Solarbio, Beijing, China). Briefly, the slides were stained with ponceau and bright green liquor to observe collagen deposition. For immunohistochemistry staining, the slides were dewaxed and rehydrated, endogenous peroxidase activity was blocked with 3% hydrogen peroxide. Antigen retrieval was by heat mediation (120°C) with citric acid (pH 5.5, Tyingbio, Nanjing, China) for 2 min. Then, non-specific antibodies were blocked by 2% bovine serum albumin (Biofroxx, Deutschland, Germany) for 1 h at room temperature. After this, the slides were incubated with primary antibodies at 4°C overnight. Negative controls were incubated with antibody dilution buffer (Tyingbio, Nanjing, China). After washing with PBS-Tween, tissues were incubated with a ready-to-use mouse/rabbit-HRP secondary antibody (Tyingbio,

Nanjing, China) for 8 min at room temperature and exposed to 3′3-diaminobenzidine to visualize the reaction sites. Images were captured by an inverted microscope (DMi8, Leica, Wetzlar, Germany). The antibodies are listed in Supplementary Table SII.

Dual-luciferase reporter gene assay

A 3′ untranslated region (3′UTR) fragment (1078-bp) of the HMGA2 containing the let-7d binding region was synthesized and purified by Generay biotechnology (Shanghai, China). Then the fragment was ligated into pGL3 dual luciferase vector (Promega, Madison, USA). IK cells at a density 5×10^5 cells per well were co-transfected with 1 μg of pGL3-HMGA2 vector and 40 pmol of let-7d mimic or antagomir (Ribobio, Guangzhou, China) using Lipofectamine 3000 (Invitrogen, Carlsbad, CA, USA). Transfection of the negative control of mimic and antagomir was also performed as a control. After 24 h, the luciferase activities of firefly and Renilla were continuously measured by a Dual Luciferase Reporter Assay kit (Vazyme). The firefly luciferase activities were normalized to the Renilla luciferase activities to calculate the relative luciferase activity of HMGA2. The sequence of let-7d mimic, antagomir and their negative control we used are as following:

miR-NC: 5′-UCACAACCUCCUAGAAAGAGUAGA-3′;
let-7d mimic: 5′-AGAGGUAGUAGGUUGCAUAGUU-3′;
antagomir-NC: 5′-UUUGUACUACACAAAAGUACUG-3′;
let-7d antagomir: 5′-AACUAUGCAACCUACUACCUCU-3′.

Overexpression plasmid and small interfering RNA (siRNA) of HMGA2

Construction of HMGA2 overexpression plasmid was synthesized by Generay biotechnology (Shanghai, China). The full length of HMGA2 (348 bp) was inserted into a pcDNA3.1 vector (pcDNA3.1-HMGA2). The pcDNA3.1 vector without sequence insertion was used as control (pcDNA3.1-ctl).

Three small interfering RNA (siRNAs) of HMGA2 and negative control (si-NC) were constructed by Ribobio (Guangzhou, China). The sequences of siRNAs as following:

si-NC: 5'-GGCUCUAGAAAAGCCUAUGCdTdT-3′;
siHMGA2 1(si-1): 5′-AGAAGCCACTGGAGAAAAA-3′;
siHMGA2 2(si-2): 5′-TGGAGAAAAACGGCCAAGA-3′;
siHMGA2 3(si-3): 5′-AGCAGAAGCCACTGGAGAA-3′.

IUA-like mouse model

All animal experiments were approved by the Institutional Animal Care and Use Committee at the Nanjing Drum Tower Hospital, Nanjing University Medical School.

Eight-week-old BALB/c female mice weighing about 20 g were purchased from the Experimental Animal Center of Nanjing Medical University (Nanjing, China) and kept in the animal room of the Nanjing Drum Tower Hospital. The IUA-like mouse model was established using dual-injury method, namely, uterine curettage and lipopolysaccharide (LPS) injection at estrus as previously described (Zhao *et al.*, 2020). Briefly, after the mice were anesthetized by inhaling isoflurane, the uterus was exposed by laparotomy. A rough-surfaced 4.5-gauge needle was inserted into the upper edge of the bilateral uterus and used to scrape it 50 times. Then a single dose of 20 μl LPS (10 mg/ml, Sigma, St. Louis, MO, USA) was injected into each uterine horn, and both ends of each uterine horn were clamped with ophthalmic forceps for 5 min. Finally, the uterus was gently brought into the abdominal cavity and the abdomen was closed. Twenty mice were randomly assigned to four groups with five mice in each group: (i) the sham group (sham), (ii) the curettage treatment group (Curettage), (iii) the agomir negative control (agomir-NC, Ribobio) treatment group (C + agomir-NC) and (iv) the let-7d agomir (agomir-let-7d, Ribobio) treatment group (C + agomir-let-7d). The sham group just received laparotomy. The treatment groups received three intrauterine injections with 20 μl PBS, agomir-NC (5 nmol) or agomir-let-7d (5 nmol) every 4 days. Endometria were collected at estrus in the fourth estrus cycle (approximately 21 days) after endometrial injury. The sequences of let-7d agomir and its negative control are as following:

agomir-NC: 5′-UCACAACCUCCUAGAAAGAGUAGA-3′;
let-7d agomir: 5′-AGAGGUAGUAGGUUGCAUAGUU-3′.

Statistics

All data were analyzed using GraphPad Prism 6.0 (USA) software and are presented as mean ± SD. Differences between two groups were analyzed using Student's *t*-test, and the difference among three or more groups was analyzed using the one-way ANOVA. $P < 0.05$ was considered a significant difference.

Results

HMGA2 is upregulated in the endometria of IUA patients and TGF-β-treated endometrial epithelial cells

The clinical information of IUA patients and the controls enrolled in this study is shown in Table I. All IUA patients enrolled in this study were diagnosed as severe IUA according to the criteria recommended by The American Fertility Society (1988) and the patients with infertility for chronic tubal obstruction but normal ovaries and endometrium were chosen as the controls. To explore the role of HMGA2 in IUA, we first assessed the expression of HMGA2 in endometria from IUA patients and the controls. The mRNA level of HMGA2 was increased by about 2.9-fold, and western blotting showed that the protein level of HMGA2 increased by about 4.6-fold in the endometria of IUA patients (Fig. 1A and B, $P < 0.0001$ and $P = 0.0095$). In order to understand the distribution of HMGA2 in endometria, we used the donors' endometria biopsy to perform HMGA2 immunohistochemical staining. Compared with normal endometria, the HMGA2 staining in endometria of IUA patients was significantly increased. Of note, HMGA2 positive foci were specifically identified in the luminal and glandular epithelium of the endometria (Fig. 1C and Supplementary Fig. S1).

We explored the expression of EMT-related genes and HMGA2 in Ishikawa cells (IK cells, an EEC line) stimulated with TGF-β. To examine whether the IK cells underwent EMT, we analyzed the expression of the epithelial marker, E-cadherin and mesenchymal markers, N-cadherin, α-smooth muscle actin (α-SMA) and fibronectin (FN). Western blotting displayed that E-cadherin protein level decreased to 67%

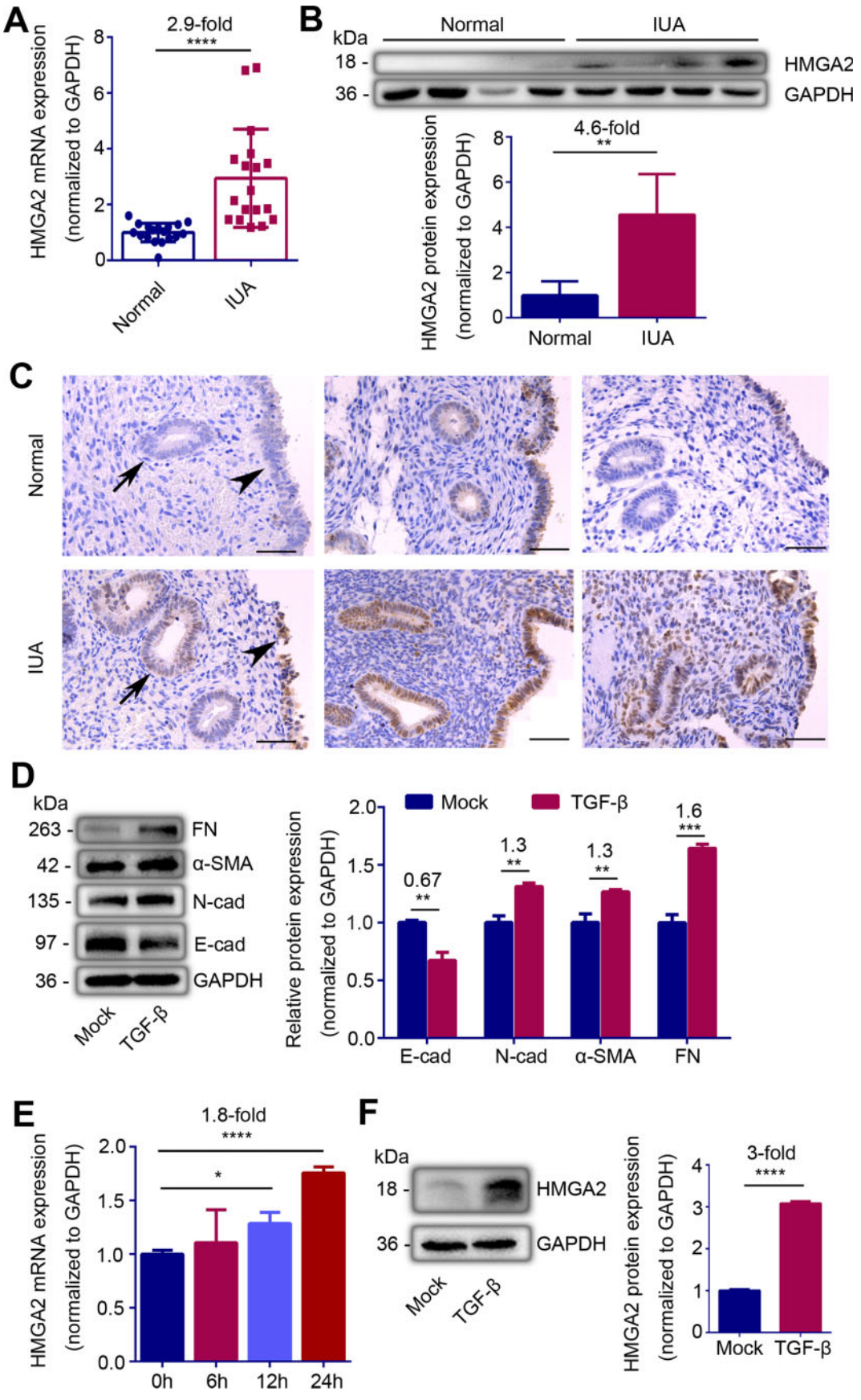

Figure 1. HMGA2 expression is abnormally upregulated in endometrial epithelial cells in intrauterine adhesions (IUA). (**A**) Relative mRNA expression of HMGA2 (n = 18), (**B**) Top: Western blot analysis of HMGA2 protein level (n = 4) and (**C**) representative

($P = 0.0014$) of the control, N-cadherin, α-SMA and FN proteins in the cells stimulated with TGF-β (10 ng/ml) were increased by 30%, 30% and 60% respectively (Fig. 1D, $P = 0.0011$, $P = 0.0038$, $P = 0.00012$). With the progress of EMT in IK cells, the mRNA level of HMGA2 increased 1.8-fold and the protein level remarkably increased by 3-fold after 24 h of TGF-β stimulation (Fig. 1E and F, $P < 0.0001$ and $P < 0.0001$).

Overexpression of HMGA2 promotes EMT and knockdown of HMGA2 prevents EMT in IK cells

To further investigate whether the specific increase of HMGA2 was directly related to EMT, we performed loss and gain of HMGA2 function in IK cells. After 48 h transfection with a high expression vector of HMGA2 (pcDNA3.1-HMGA2), the mRNA and protein levels of HMGA2 increased by12.5-fold and 2-fold, respectively (Fig. 2A and B, $P < 0.0001$ and $P < 0.0001$). With the increment of HMGA2, expression levels of N-cadherin, α-SMA, and FN were enhanced by 20%, 40% and 120%, respectively ($P = 0.01$, $P = 0.0031$ and $P = 0.0007$), while the level of E-cadherin was decreased by 45% (Fig. 2C, $P = 0.0011$). These results indicated that HMGA2 promoted EMT. We also constructed three small interference sequences of HMGA2 (si-1, si-2, si-3) to knockdown of HMGA2. The results showed that transfection si-3 can reduce the mRNA level of HMGA2 by 62% and the protein level by 85% (Fig. 2D and E, $P = 0.0035$ and $P < 0.0001$). Thus, we selected the si-3 for subsequent experiments because it exerted the greatest interference effect. After knockdown of HMGA2 with si-3, E-cadherin protein expression upregulated by 15% ($P = 0.0086$), while N-cadherin, α-SMA and FN protein expression downregulated to 66%, 54% and 58%, respectively (Fig. 2F, $P = 0.0004$, $P = 0.0003$ and $P = 0.0005$). Furthermore, we transfected si-HMGA2 into IK cells pre-stimulated with TGF-β for 24 h. After transfection for 48 h, E-cadherin protein level rebounded by 20% ($P = 0.002$), while N-cadherin, α-SMA and FN protein expression downregulated by 26%, 74% and 56%, respectively (Fig. 2G, $P = 0.002$, $P < 0.0001$ and $P = 0.0001$), which suggested that the EMT process of IK cells induced by TGF-β was reversed. These results confirmed that HMGA2 directly mediated EMT and inhibition of HMGA2 can prevent EMT.

let-7d is downregulated in endometrium of IUA patients and prevents EMT induced by TGF-β in IK cells

To understand the role of let-7d in the processes of IUA, we examined the level of let-7d in endometria. The results revealed that the expression of let-7d in the endometria of IUA patients was significantly lower than that in normal endometria (Fig. 3A, $P < 0.0001$). We further detected the let-7d level in IK cells stimulated by TGF-β and found that expression level of let-7d decreased by 42% after 24 h stimulation (Fig. 3B, $P = 0.047$). Given that the pro-EMT effect of TGF-β and the reported anti-EMT effect of let-7d, we transfected let-7d mimic to promote re-expression of let-7d in IK cells pre-treated by TGF-β. The results showed that supplementing let-7d reversed the EMT caused by TGF-β, resulting in a rise in E-cadherin (Fig. 3C and F, $P = 0.01$ and $P < 0.0001$), and a decline in N-cadherin (Fig. 3F, $P = 0.0008$), α-SMA (Fig. 3D and F, $P = 0.0012$ and $P = 0.0002$) and FN (Fig. 3E and F, $P = 0.0372$ and $P = 0.0072$) levels.

Let-7d inhibits HMGA2 expression and HMGA2 induced EMT in IK cells

Since let-7d and HMGA2 showed opposite effects in IUA, we further explored their targeting relationship in IK cells. We first transfected let-7d mimic and antagomir in IK cells, and found that let-7d level in IK cells increased by 40-fold after let-7d mimic transfection while it reduced to 50% after let-7d antagomir transfection (Fig. 4A, $P = 0.0222$ and $P = 0.0025$). In line with the prediction, the luciferase activity of HMGA2 was decreased by 73% after let-7d mimic transfection and was increased by 3-fold after let-7d antagomir transfection (Fig. 4B, $P = 0.0053$ and $P < 0.0001$). Meanwhile, the high expression of let-7d inhibited the expression of HMGA2, resulting in a 20% decrease in HMGA2 mRNA level and a 57% decrease in protein level (Fig. 4C and D, $P = 0.0032$ and $P < 0.0001$). Knockdown of let-7d resulted in a 330% and 80% increase in HMGA2 mRNA and protein level, respectively (Fig. 4C and D, $P < 0.0001$ and $P = 0.0035$). We also showed that let-7d mimic counteracted the upregulation of HMGA2 induced by TGF-β in IK cells (Fig. 4E and F, $P = 0.0014$ and $P = 0.0007$). Furthermore, let-7d mimic reversed HMGA2 induced EMT in IK cells, with increment of E-cadherin ($P = 0.0003$), and decrement of N-cadherin, α-SMA and FN (Fig. 4G, $P = 0.0002$, $P = 0.0024$ and $P = 0.0005$). These results suggested that let-7d directly targeted HMGA2.

Overexpression of let-7d suppresses HMGA2 expression and EEC-EMT in IUA-like mouse model

Consistent with the evidence in human endometria, let-7d expression was downregulated to 27% of the sham-operated mice (Fig. 5A, $P = 0.0283$) and HMGA2 mRNA expression was upregulated by 90% in endometria of the IUA-like mouse model compared with that of

Figure 1. Continued

immunohistochemistry images of HMGA2 ($n = 3$) in endometria of normal controls and severe IUA patients. Scale bars, 50 μm. Arrow head: luminal epithelial cells; arrow: glandular epithelial cells. (**D**) Left: western blot analysis of E-cadherin (E-cad), N-cadherin (N-cad), α-smooth muscle actin (α-SMA) and fibronectin (FN) proteins levels in TGF-β-treated Ishikawa (IK) cells. (**E**) Relative mRNA expression of HMGA2 in TGF-β-treated IK cells at the indicated point of time ($n = 3$). (**F**) Left: western blot analysis of HMGA2 protein level in IK cells treated by TGF-β for 24 h. (**B**) Bottom and (**F**) Right: quantification of corresponding bands ($n = 3$) determined by image J software. The data are shown as the mean ± SD. *$P < 0.05$; **$P < 0.01$; ***$P < 0.001$; ****$P < 0.0001$. Student's *t*-tests were performed for panels A, B, D and F. For panel E, one-way ANOVA was performed. The number above the asterisk in each panel is the fold difference.

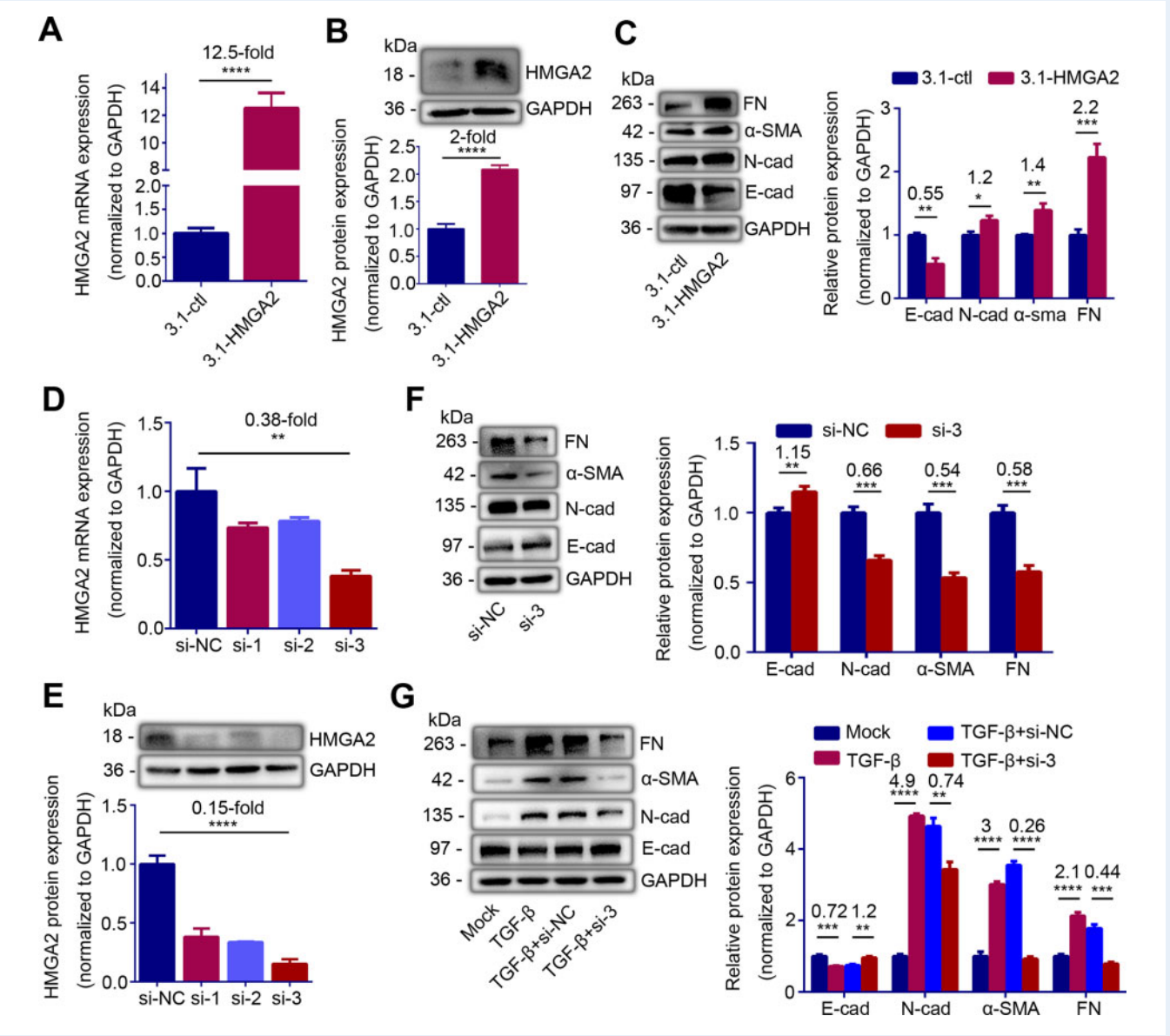

Figure 2. HMGA2 contributes to epithelial-mesenchymal transition (EMT) of endometrial epithelial cells. (**A**) HMGA2 mRNA level ($n = 5$) and (**B**) Left: western blot analysis of HMGA2 protein level in Ishikawa (IK) cells transfected with HMGA2 high expression plasmid or control plasmid for 24 h. (**C**) Left: western blot analysis of E-cadherin (E-cad), N-cadherin (N-cad), α-smooth muscle actin (α-SMA) and fibronectin (FN) proteins levels in IK cells transfected with HMGA2 high expression plasmid or control plasmid for 48 h. (**D**) HMGA2 mRNA expression ($n = 3$), and (**E**) Top: western blot analysis of HMGA2 protein level in IK cells transfected with different small interfering RNAs of HMGA2 (si-1, si-2, si-3) or negative control (si-NC) for 24 h. (**F**) Left: western blot analysis of E-cad, N-cad, α-SMA and FN proteins levels in IK cells transfected with si-HMGA2 or si-NC for 48 h. (**G**) Left: western blot analysis of E-cad, N-cad, α-SMA and FN proteins levels in TGF-β-pretreated IK cells transfected with si-HMGA2 (TGF-β + si-3) or si-NC (TGF-β + si-NC) for 48 h. (**C**, **F**, **G**) Right and **(E)** Bottom: quantification of corresponding proteins ($n = 3$) determined by image J software. The data are shown as the mean ± SD. *$P < 0.05$; **$P < 0.01$; ***$P < 0.001$; ****$P < 0.0001$. Student's *t*-tests were performed for all panels. The number above the asterisk in each panel is the fold difference.

the sham-operated mice (Fig. 5B, $P = 0.0010$). HMGA2 immunohistochemical staining showed that HMGA2 positive staining is mainly located in EECs of the IUA-like mouse model, which was consistent to the results in endometria of IUA patients (Fig. 5C and Supplementary Fig. S2). The mouse model also exhibited decreases in endometrial glands and the expression of E-cadherin and increases in N-cadherin and α-SMA expression as well as the accumulation of collagen protein evidenced by positive Masson staining (Fig. 5C).

The injection of let-7d agomir into the uterine cavity of IUA-like mouse model resulted in overexpression of let-7d (Fig. 5A, $P = 0.047$). With the replenishment of let-7d, HMGA2 mRNA ($P = 0.0411$) and protein expression were inhibited (Fig. 5B and C). Furthermore, the

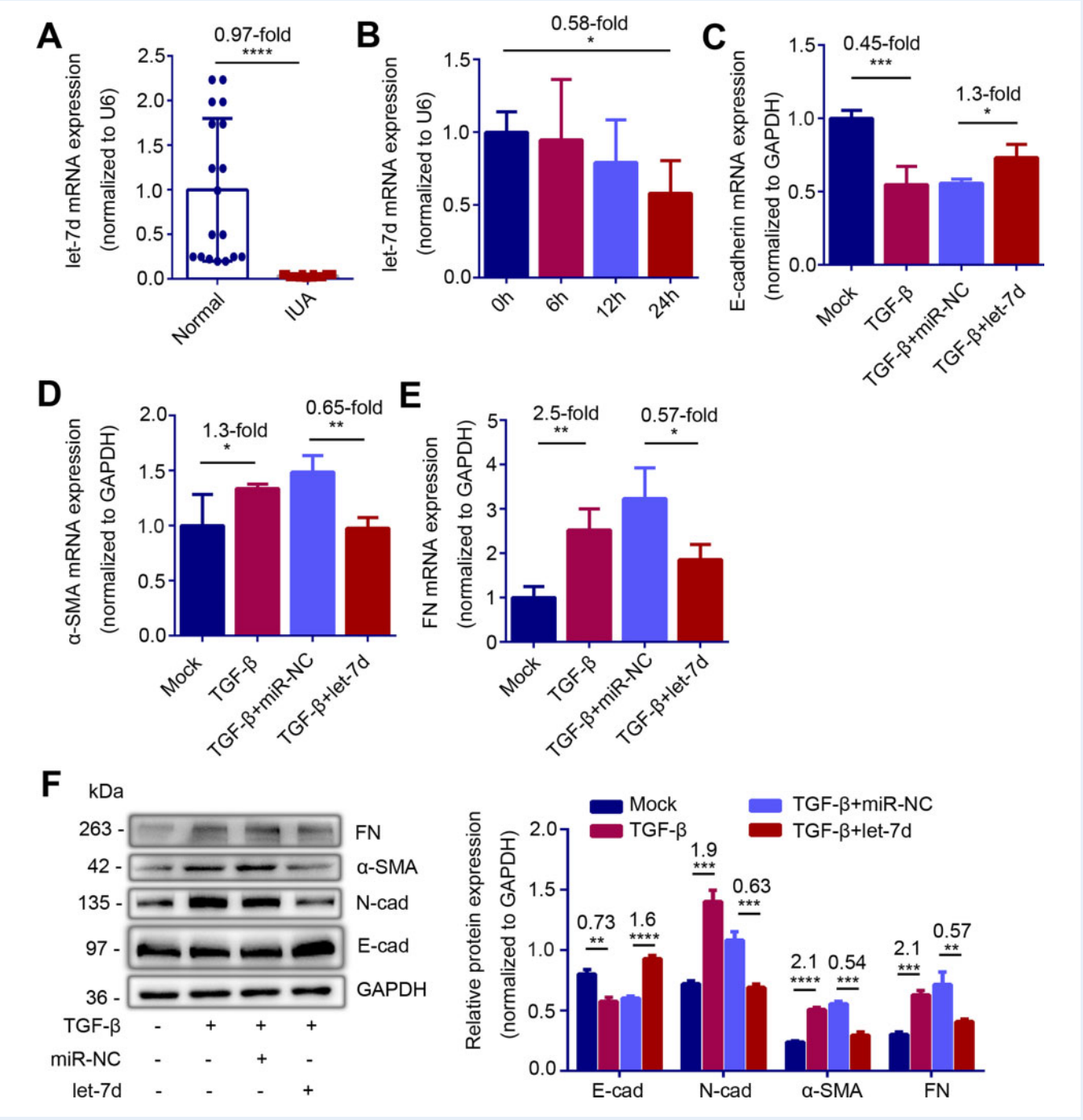

Figure 3. let-7d is downregulated in endometria of intrauterine adhesions (IUA) patients and prevents epithelial–mesenchymal transition (EMT) *in vitro*. (**A**) Relative expression of let-7d in endometria of normal controls ($n = 18$) and severe IUA patients ($n = 18$). (**B**) Relative expression of let-7d in TGF-β-treated Ishikawa (IK) cells at the indicated point of time ($n = 3$). (**C**) Relative mRNA expression of E-cad ($n = 4$), (**D**) α-SMA ($n = 4$), (**E**) FN ($n = 4$) and (**F**) Left: western blot analysis of E-cad, N-cad, α-SMA and FN proteins levels in TGF-β-pretreated IK cells transfected with let-7d mimic (TGF-β + let-7d) or microRNA negative control (TGF-β + miR-NC) for 48 h. Right: Quantification of corresponding proteins ($n = 3$) determined by image J software. The data are shown as the mean ± SD. *$P < 0.05$; **$P < 0.01$; ***$P < 0.001$; ****$P < 0.0001$. Student's *t*-tests were performed for panels A, C to F. For panel B, one-way ANOVA was performed. The number above the asterisk in each panel is the fold difference.

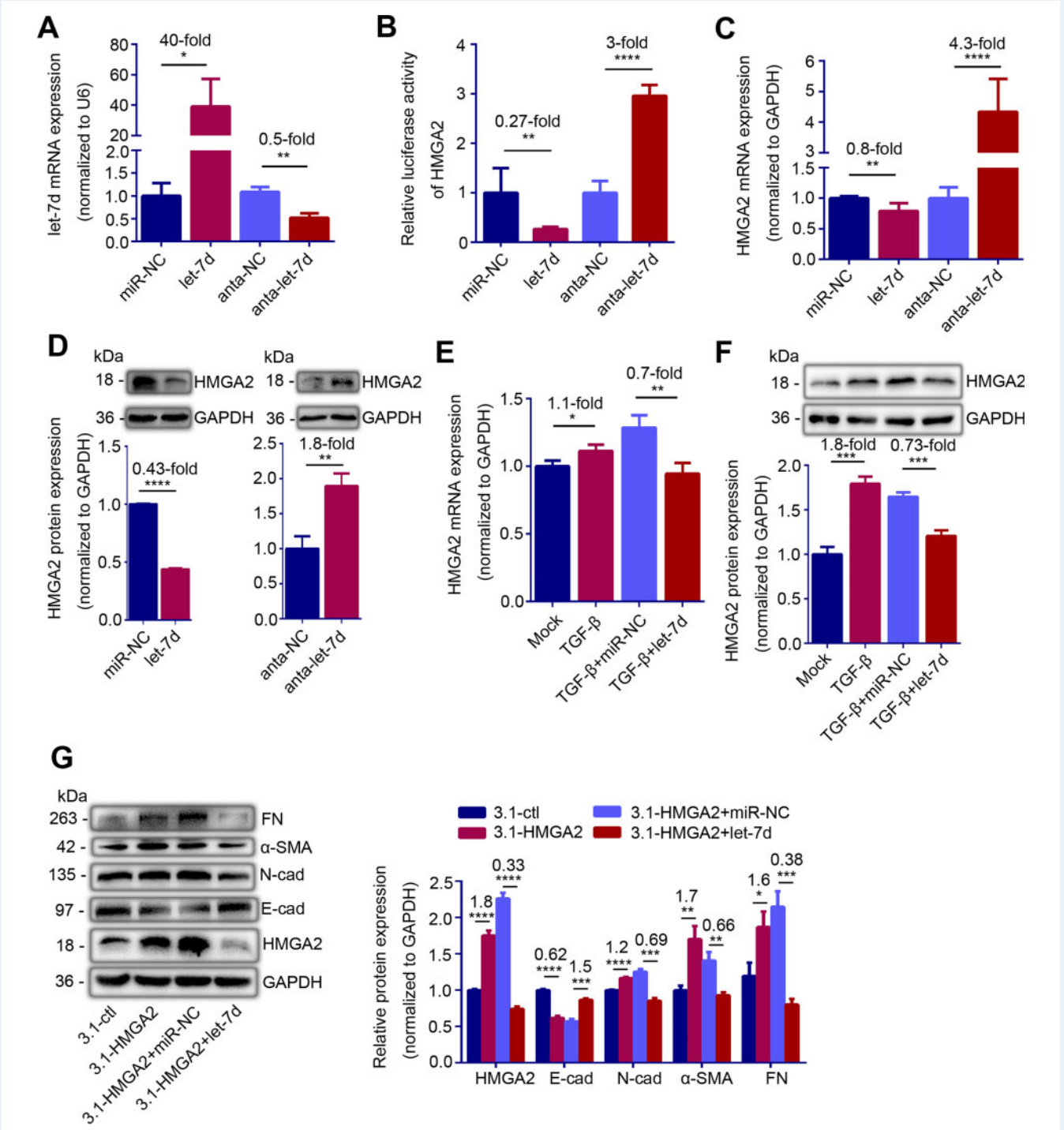

Figure 4. let-7d represses HMGA2 expression and HMGA2-induced epithelial–mesenchymal transition (EMT) *in vitro*. (**A**) let-7d mRNA level ($n = 3$), (**B**) Luciferase activity of HMGA2 ($n = 6$), (**C**) HMGA2 mRNA level ($n = 3$) and (**D**) Top: HMGA2 protein level in IK cells transfected with miR-NC, let-7d mimic, antagomir negative control (anta-NC) or let-7d antagomir (anta-let-7d) for 24 h. (**E**) HMGA2 mRNA level ($n = 3$) and (**F**) Top: HMGA2 protein level in TGF-β-pretreated IK cells transfected with miR-NC or let-7d mimic for 48 h. (**G**) Left: Western blot analysis of E-cad, N-cad, α-SMA and FN proteins levels in IK cells transfected with let-7d mimic or miR-NC for 48 h in the presence of HMGA2 high expression plasmid. (**D**) Bottom, (**F**) Bottom and (**G**) Right: Quantification of corresponding proteins ($n = 3$) determined by image J software. The data are shown as the mean ± SD. $^{*}P < 0.05$; $^{**}P < 0.01$; $^{***}P < 0.001$; $^{****}P < 0.0001$. Student's *t*-tests were performed for all panels. The number above the asterisk in each panel is the fold difference.

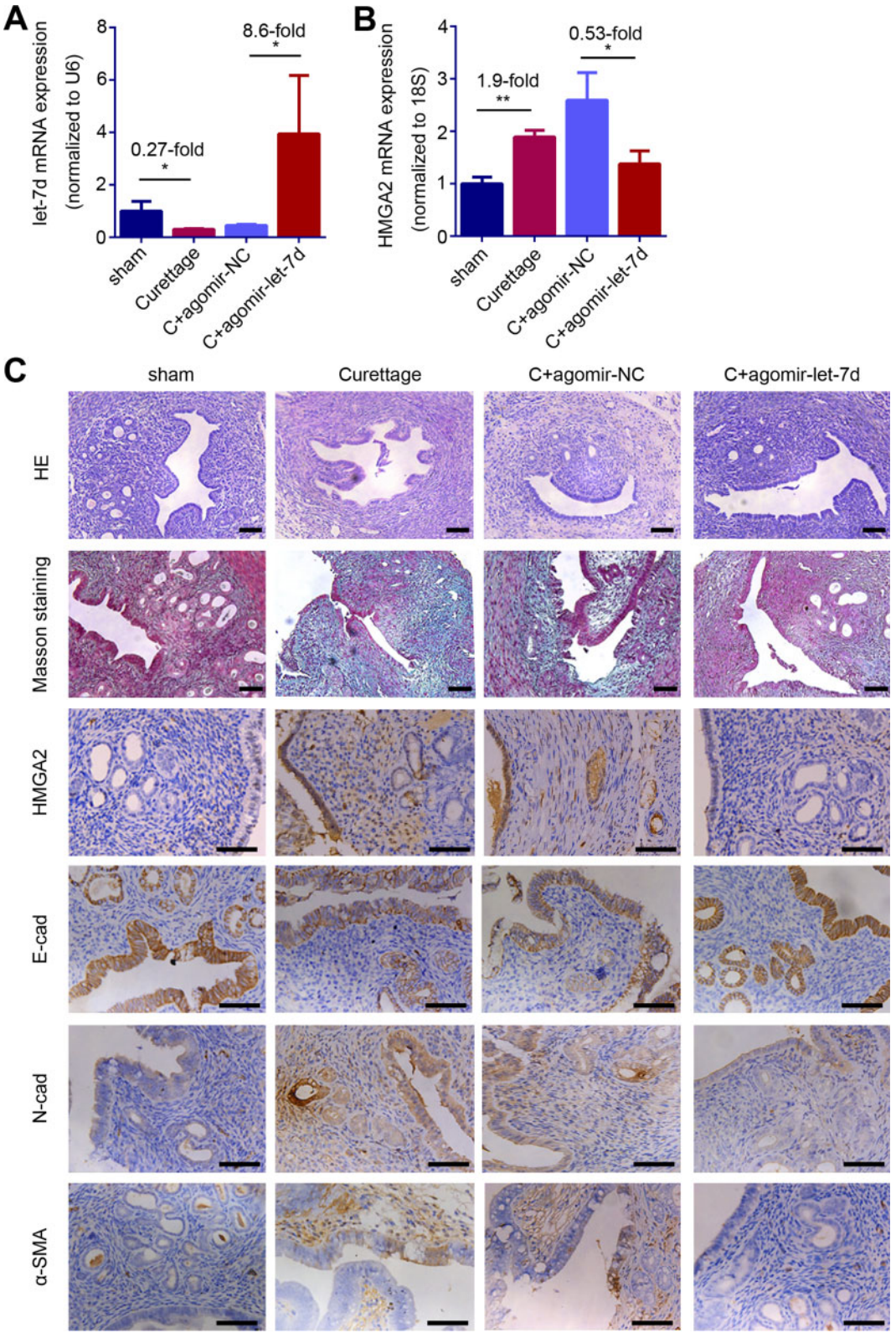

Figure 5. let-7d inhibits HMGA2 expression and prevents epithelial–mesenchymal transition (EMT) in intrauterine adhesions (IUA)-like mouse. (**A**) let-7d mRNA level, (**B**) HMGA2 mRNA level and (**C**) Representative images of HE, Mason staining, HMGA2, E-cad, N-cad and α-SMA in mice endometrial biopsies of the sham ($n = 5$), the curettage treatment ($n = 5$), the curettage with agomir negative control (C + agomir-NC, $n = 5$) treatment and the curettage with let-7d agomir (C + agomir-let-7d, $n = 5$) treatment group. Scale bars, 50 μm. The data are shown as the mean ± SD. *$P < 0.05$; **$P < 0.01$. Student's *t*-tests were performed for panel A and B. The number above the asterisk in each panel is the fold difference.

mice treated with let-7d agomir had functionally regenerated endometrium, with increased E-cadherin, decreased N-cadherin and α-SMA, and less collagen deposition compared to the mouse model treated with agomir negative control (agomir-NC, Fig. 5C).

Discussion

An important histological feature of IUA is endometrial fibrosis. EMT is an important driver of endometrium fibro-genesis, but the molecular mechanism involved is still not well understood. In this study, we demonstrate that HMGA2 was significantly upregulated while let-7d was downregulated in the endometria of severe IUA patients and TGF-β-treated IK cells. We further found that HMGA2 promoted EEC-EMT and let-7d can target HMGA2 to protect EEC from EMT.

HMGA2 is a multifunctional regulator involved in development, differentiation, stemness, tumorigenesis and fibrogenesis, and its direct or indirect regulation in EMT is an important aspect of its participation in the progress of these physiologic and pathologic conditions (Fusco and Fedele, 2007; Fedele and Fusco, 2010; Vignali *et al.*, 2020). HMGA2 is highly expressed in fetal tissue but rarely expressed in normal adult tissues (Rogalla *et al.*, 1996). In terms of endometrial diseases, HMGA2 is found to be overexpressed in epithelial tumors. Ectopic expressed HMGA2 promotes EMT in early stage of endometrioid endometrial carcinoma and is considered to be a useful biomarker of endometrial serous adenocarcinoma (McCluggage *et al.*, 2012; Wei *et al.*, 2016). HMGA2 overexpression in uterine fibroids has also been reported by several researchers (Mehine *et al.*, 2016; Äyräväinen *et al.*, 2020). Recently, an integrated epigenome, exome and transcriptome analyses revealed that HMGA1 and HMGA2 overexpression is observed in approximately 20–30% of all fibroids. Upregulation of HMGA2 expression may be attributed to rearrangements at 12q14-15 and DNA hypomethylation in the HMGA2 gene body (George *et al.*, 2019). HMGA2 plays important role in benign and malignant endometrial proliferation diseases, but its role in IUA, a disease with endometrial dysplasia, has not been studied. The present study establishes the role of HMGA2 in endometrial fibrosis and reveals that the upregulation of HMGA2 in endometria of IUA patients is mainly located in EECs. IK cells are derived from a well-differentiated, minimal-invasive human endometrial adenocarcinoma, and are responsive to estradiol; they have both estrogen and inducible progesterone receptors (Nishida *et al.*, 1985). They have moderate apicobasal polarity and steroid responsiveness similar to EECs (Heneweer *et al.*, 2005; Kakar-Bhanot *et al.*, 2019), leading us to select IK cells to perform experiments *in vitro*. We confirmed that high expression of HMGA2 promoted EMT and knocking out HMGA2 reversed EMT. TGF-β is one of the most important mediators of tissue fibrosis and a crucial inducer of EMT (Kopp, 2010; Yeh *et al.*, 2010; Yang *et al.*, 2012; Wang *et al.*, 2018) and silencing HMGA2 also inhibited TGF-β-induced EMT in IK cells.

The activity of HMGA can be post-transcriptionally regulated, and microRNAs play an important role (Hammond and Sharpless, 2008; Sgarra *et al.*, 2009; Zhang and Wang, 2010). Liu *et al.* (2016) reported that miR-23b targets HMGA2 to suppress EMT in diabetic nephropathy and Chen *et al.* (2020) reported that miR-26b targets HMGA2 to ameliorate myocardial infarction-induced fibrosis by suppression of cardiac fibroblasts activation. It has also been reported that let-7d can regulate the expression of HMGA2 (Wang *et al.*, 2016a,b). Let-7d is a member of the let-7 family and is considered to be involved in EMT process of some fibrotic diseases (Nam *et al.*, 2011; Wang *et al.*, 2016a,b). In searching how is HMGA2 expression regulated in IUA, we found that let-7d can target to the 3′UTR of HMGA2 to inhibit its expression and functionally reversed HMGA2-induced EMT.

Published IUA modeling procedures are diverse but mechanical injury mixed with administration of LPS (dual-injury mouse model) provokes typical EEC-EMT (Sun *et al.*, 2019; Zhao *et al.*, 2020), thus we choose this modeling method. Dual injury resulted in a decrease in E-cadherin, and increases in the mesenchymal markers, N-cadherin, α-SMA and FN and fibrosis degree in the endometria of mice. These data indicate that the dual-injury model can successfully induce EEC-EMT, leading to endometrial fibrosis as previously reported. Consistent with the *ex vivo* results, the expression of HMGA2 in the endometria of IUA-like mice was significantly increased, while the expression of let-7d was decreased. When let-7d was supplemented, HMGA2 expression was repressed, and EEC-EMT was reversed, ameliorating dual-injury-induced endometrial fibrosis.

In summary, our study highlights the interaction of let-7d/HMGA2 in endometria of IUA patients and provides new insight into the development of potential therapeutic targets for IUA.

Supplementary data

Supplementary data are available at *Molecular Human Reproduction* online.

Data availability

The raw data that support the fndings of this study are available from the corresponding author on reasonable request.

Acknowledgements

We thank Jingmei Wang for biopsy diagnosis of endometrium tissue. We thank Chenyan Dai for the ultrasound examination of normal controls and IUA patients.

Authors' roles

Y.H. designed the study and revised the paper. G.Z. instructed experiments and helped to write the paper. M.S. carried out the experiments and wrote the paper. C.C. helped with the IUA-like mouse model construction. Z.Z. and S.Y. contributed to analyze the results. P.J. helped to collect the samples of endometria. H.W. performed hysteroscopic biopsy. All authors discussed the results and commented on the manuscript.

Funding

This study was supported by research grants from the Strategic Priority Research Program of the Chinese Academy of Sciences (XDA16040300), National Natural Science Foundation of China (81771526, 81971336, 82071600) and Jiangsu Province's Key Provincial Talents Program (ZDRCA2016067).

Conflict of interest

The authors declare no conflict of interests.

References

Ai Y, Chen M, Liu J, Ren L, Yan X, Feng Y. lncRNA TUG1 promotes endometrial fibrosis and inflammation by sponging miR-590-5p to regulate Fasl in intrauterine adhesions. *Int Immunopharmacol* 2020; **86**:106703.

Al-Inany H. Intrauterine adhesions. An update. *Acta Obstet Gynecol Scand* 2001;**80**:986–993.

Äyräväinen A, Pasanen A, Ahvenainen T, Heikkinen T, Pakarinen P, Härkki P, Vahteristo P. Systematic molecular and clinical analysis of uterine leiomyomas from fertile-aged women undergoing myomectomy. *Hum Reprod* 2020;**35**:2237–2244.

Chen X, Ding Z, Li T, Jiang W, Zhang J, Deng X. MicroR-26b targets high mobility group, AT-hook 2 to ameliorate myocardial infarction-induced fibrosis by suppression of cardiac fibroblasts activation. *Curr Neurovasc Res* 2020;**17**:204–213.

Fedele M, Fusco A. HMGA and cancer. *Biochim Biophys Acta* 2010; **1799**:48–54.

Fusco A, Fedele M. Roles of HMGA proteins in cancer. *Nat Rev Cancer* 2007;**7**:899–910.

George JW, Fan H, Johnson B, Carpenter TJ, Foy KK, Chatterjee A, Patterson AL, Koeman J, Adams M, Madaj ZB *et al*. Integrated epigenome, exome, and transcriptome analyses reveal molecular subtypes and homeotic transformation in uterine fibroids. *Cell Rep* 2019;**29**:4069–4085.e6.

Hammond SM, Sharpless NE. HMGA2, microRNAs, and stem cell aging. *Cell* 2008;**135**:1013–1016.

Heneweer C, Schmidt M, Denker HW, Thie M. Molecular mechanisms in uterine epithelium during trophoblast binding: the role of small GTPase RhoA in human uterine Ishikawa cells. *J Exp Clin Assist Reprod* 2005;**2**:4.

Hooker AB, Lemmers M, Thurkow AL, Heymans MW, Opmeer BC, Brolmann HAM, Mol BW, Huirne JAF. Systematic review and meta-analysis of intrauterine adhesions after miscarriage: prevalence, risk factors and long-term reproductive outcome. *Hum Reprod Update* 2014;**20**:262–278.

Hou M, Bao X, Luo F, Chen X, Liu L, Wu M. HMGA2 modulates the TGFβ/Smad, TGFβ/ERK and Notch signaling pathways in human lens epithelial-mesenchymal transition. *Curr Mol Med* 2018;**18**:71–82.

Kakar-Bhanot R, Brahmbhatt K, Chauhan B, Katkam RR, Bashir T, Gawde H, Mayadeo N, Chaudhari UK, Sachdeva G. Rab11a drives adhesion molecules to the surface of endometrial epithelial cells. *Hum Reprod* 2019;**34**:519–529.

Kopp JB. TGF-beta signaling and the renal tubular epithelial cell: too much, too little, and just right. *JASN* 2010;**21**:1241–1243.

Liu H, Wang X, Liu S, Li H, Yuan X, Feng B, Bai H, Zhao B, Chu Y, Li H. Effects and mechanism of miR-23b on glucose-mediated epithelial-to-mesenchymal transition in diabetic nephropathy. *Int J Biochem Cell Biol* 2016;**70**:149–160.

Macrì S, Simula L, Pellarin I, Pegoraro S, Onorati M, Sgarra R, Manfioletti G, Vignali R. Hmga2 is required for neural crest cell specification in Xenopus laevis. *Dev. Biol* 2016;**411**:25–37.

March CM. Asherman's syndrome. *Semin Reprod Med* 2011b;**29**:83–94.

March CM. Management of Asherman's syndrome. *Reprod BioMed Online* 2011a;**23**:63–76.

McCluggage WG, Connolly LE, McBride HA, Kalloger S, Gilks CB. HMGA2 is commonly expressed in uterine serous carcinomas and is a useful adjunct to diagnosis. *Histopathology* 2012;**60**:547–553.

Mehine M, Kaasinen E, Heinonen H-R, Mäkinen N, Kämpjärvi K, Sarvilinna N, Aavikko M, Vähärautio A, Pasanen A, Bützow R *et al*. Integrated data analysis reveals uterine leiomyoma subtypes with distinct driver pathways and biomarkers. *Proc Natl Acad Sci USA* 2016;**113**:1315–1320.

Nam Y, Chen C, Gregory Richard I, Chou James J, Sliz P. Molecular basis for interaction of let-7 microRNAs with Lin28. *Cell* 2011; **147**:1080–1091.

Nishida M, Kasahara K, Kaneko M, Iwasaki H, Hayashi K. Establishment of a new human endometrial adenocarcinoma cell line, Ishikawa cells, containing estrogen and progesterone receptors. *Nihon Sanka Fujinka Gakkai Zasshi* 1985;**37**:1103–1111.

Rogalla P, Drechsler K, Frey G, Hennig Y, Helmke B, Bonk U, Bullerdiek J. HMGI-C expression patterns in human tissues. Implications for the genesis of frequent mesenchymal tumors. *Am J Pathol* 1996;**149**:775–779.

Salazar CA, Isaacson K, Morris S. A comprehensive review of Asherman's syndrome: causes, symptoms and treatment options. *Curr Opin Obstet Gynecol* 2017;**29**:249–256.

Sgarra R, Maurizio E, Zammitti S, Lo Sardo A, Giancotti V, Manfioletti G. Macroscopic differences in HMGA oncoproteins post-translational modifications: C-terminal phosphorylation of HMGA2 affects its DNA binding properties. *J Proteome Res* 2009; **8**:2978–2989.

Sun L, Zhang S, Chang Q, Tan J. Establishment and comparison of different intrauterine adhesion modelling procedures in rats. *Reprod Fertil Dev* 2019. In Press

The American Fertility Society Classifications of Adnexal Adhesions, distal tubal occlusion, secondary to tubal ligation, tubal pregnancies, mullerian anomalies and intrauterine adhesions. *Fertil Steril* 1988;**49**:944–955.

Vignali R, Marracci S.HMGA Genes and Proteins in Development and Evolution. IJMS 2020;**21**:654 10.3390/ijms21020654

Wang P, Luo M, Song E, Zhou Z, Ma T, Wang J, Jia N, Wang G, Nie S, Liu Y *et al*. lnc-TSI Long noncoding RNA inhibits renal fibrogenesis by negatively regulating the TGF-β/Smad3 pathway. *Sci Transl Med* 2018 ;10.:eaat2039.

Wang Y, Le Y, Xue J, Zheng Z, Xue Y. Let-7d miRNA prevents TGF-β1-induced EMT and renal fibrogenesis through regulation of HMGA2 expression. *Biochem Biophys Res Commun* 2016a;**479**:676–682.

Wang Y, Liu J, Tang H, Nie J, Zhu J, Wen L, Guo Q. miR-221 targets HMGA2 to inhibit bleomycin-induced pulmonary fibrosis by regulating TGF-β1/Smad3-induced EMT. *Int J Mol Med* 2016b;**38**: 1208–1216.

Wei L, Liu X, Zhang W, Wei Y, Li Y, Zhang Q, Dong R, Kwon JS, Liu Z, Zheng W *et al*. Overexpression and oncogenic function of HMGA2 in endometrial serous carcinogenesis. *Am J Cancer Res* 2016;**6**:249–259.

Yang S, Banerjee S, de Freitas A, Sanders YY, Ding Q, Matalon S, Thannickal VJ, Abraham E, Liu G. Participation of miR-200 in pulmonary fibrosis. *Am J Pathol* 2012;**180**: 484–493.

Yeh Y, Wei W, Wang Y, Lin S, Sung J, Tang M. Transforming growth factor-beta1 induces Smad3-dependent beta1 integrin gene expression in epithelial-to-mesenchymal transition during chronic tubulointerstitial fibrosis. *Am J Pathol* 2010;**177**:1743–1754.

Yu D, Wong Y, Cheong Y, Xia E, Li T. Asherman syndrome–one century later. *Fertil Steril* 2008;**89**:759–779.

Zhang Q, Wang Y. HMG modifications and nuclear function. *Biochim Biophys Acta* 2010;**1799**:28–36.

Zhao G, Li R, Cao Y, Song M, Jiang P, Wu Q, Zhou Z, Zhu H, Wang H, Dai C *et al.* ΔNp63α-induced DUSP4/GSK3β/SNAI1 pathway in epithelial cells drives endometrial fibrosis. *Cell Death Dis* 2020;**11**:449.

Zhu Y, Xu J, Liang W, Li J, Feng L, Zheng PXi, Ji T, Bai S. miR-98-5p alleviated epithelial-to-mesenchymal transition and renal fibrosis via targeting Hmga2 in diabetic nephropathy. *Int J Endocrinol* 2019; **2019**:4946181.